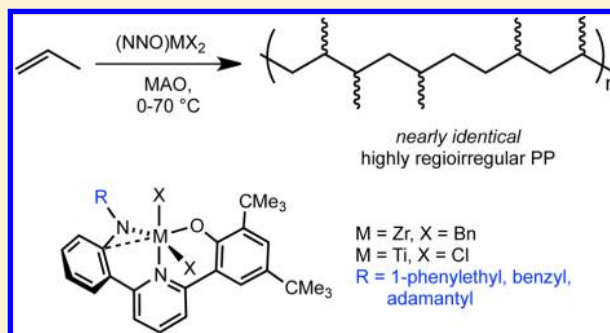


Investigations into Asymmetric Post-Metallocene Group 4 Complexes for the Synthesis of Highly Regioirregular Polypropylene

Rachel C. Klet,[†] Curt N. Theriault,[‡] Jerzy Klosin,[‡] Jay A. Labinger,^{*,†} and John E. Bercaw^{*,†}[†]Arnold and Mabel Beckman Laboratories of Chemical Synthesis, California Institute of Technology, Pasadena, California 91125, United States[‡]Corporate R&D, The Dow Chemical Company, 1776 Building, Midland, Michigan 48674, United States

S Supporting Information

ABSTRACT: A series of asymmetric post-metallocene group 4 complexes based on a modular anilide(pyridine)phenoxide framework have been synthesized and tested for propylene polymerization activity. These complexes, upon activation with methylaluminoxane (MAO), produce highly regioirregular and stereoirregular polypropylene with moderate to good activities. Surprisingly, modification of the anilide R-group substituent from 1-phenethyl to benzyl or adamantyl did not significantly change the polymer microstructure as determined by ¹³C NMR spectroscopy. Although polymer molecular weights and polydispersities vary with propylene pressure, temperature, and activator, regio- and stereoirregularity were also found to be relatively insensitive to these variables. When the polymerization is conducted at 70 °C under dihydrogen, partial decomposition to a highly active catalyst that produces an isotactic microstructure occurs; the undecomposed catalyst continues to produce highly regioirregular and stereoirregular polypropylene under these conditions.

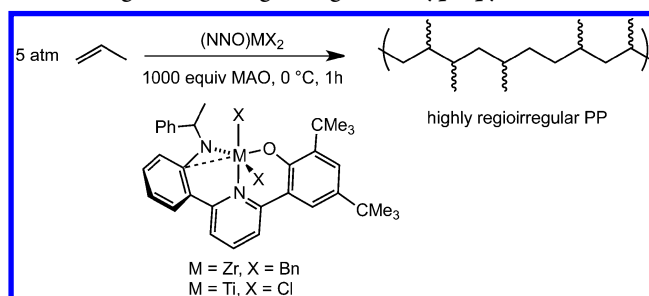


1. INTRODUCTION

Polyolefins are one of the most important classes of synthetic polymers.¹ Decades after the discovery of Ziegler–Natta catalysts for producing polyethylenes and polypropylenes,² single-sited homogeneous catalytic systems were described. The development of metallocene catalysts in the 1980s led to significant advances in our understanding of how catalyst structure affects the polymer microstructure.³ More recently, the rise of “post-metallocene” olefin polymerization catalysts has led to the realization of new polymer architectures and significant innovations in living polymerization.⁴

We have reported group 4 complexes having triaromatic dianionic (XLX) pincer ligands of the type anilide(pyridine)-phenoxide (NNO), which upon activation with methylaluminoxane (MAO) polymerize propylene with good activities (Scheme 1).⁵ These catalysts follow previous work in our group to develop olefin polymerization catalysts based on triaromatic dianionic (XLX) pincer ligands, including bis(phenolate) ligands with pyridine (ONO), furan (OOO) and thiophene (OSO) linkers, and bis(anilide)pyridine ligands (NNN).^{6–8} Significantly, the polypropylene produced by asymmetric NNO complexes is highly regioirregular, while propylene produced by complexes with symmetric triaromatic ligands is regioregular. In fact, we have determined that as many as 30–40% of enchainments may be inverted to a 2,1-insertion mode in polypropylene produced by NNO complexes. This observed lack of regiocontrol is very unusual for an early metal polymerization catalyst and warrants further study to elucidate

Scheme 1. Propylene Polymerization with Group 4 Anilide(Pyridine)Phenoxide (NNO) Complexes Yields Stereoirregular and Regioirregular Polypropylene



its origin. Herein we report our studies aimed at revealing the origins of the lack of regiocontrol exhibited by asymmetric group 4 NNO complexes.

2. RESULTS AND DISCUSSION

Anilide R-Group Variations. Our initial ligand design L1 included a chiral 1-phenylethyl group on the anilide arm, resulting in a C₁-symmetric ligand and precatalyst (Figure 1). The NNO ligand was designed to be easily variable at the anilide R-group, and given the proximity of this group to the

Received: February 28, 2014

Revised: April 28, 2014

Published: May 14, 2014



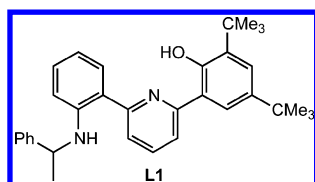
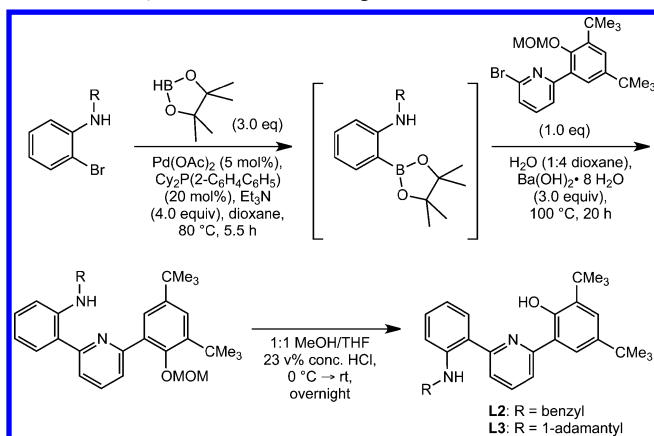


Figure 1. Ligand L1.

metal center, it was expected to influence the stereochemistry of incoming α -olefin monomers. We reasoned one potential origin of regioerrors could be the interactions of the incoming monomer with the chiral group on the ligand arm. To probe the effect of this group on regiocontrol, we sought to make C_s -symmetric ligands having achiral anilide R-groups. Ligands **L2** and **L3**, with benzyl and adamantyl groups, respectively, were synthesized using synthetic procedures similar to that reported for the synthesis of **L1** (Scheme 2).⁵

Scheme 2. Synthesis of NNO Ligand Variants L2 and L3



Metalation of the new NNO ligand variants **L2** and **L3** was achieved through protonolytic release of either 2 equiv of toluene with tetrabenzylzirconium or of 2 equiv of dimethylamine with $\text{TiCl}_2(\text{NMe}_2)_2$ to yield (**L2**) ZrBn_2 **1**, (**L2**) TiCl_2 **2**, and (**L3**) TiCl_2 **3** (Scheme 3).

Crystals of **1** suitable for X-ray diffraction were grown from a concentrated pentane solution at 35 °C (Figure 2). The crystal structure of **1** is similar to the previously reported structure of (**L1**) TiCl_2 **4**.⁵ Both complexes have distorted trigonal-bipyramidal geometry, and the anilide arm is noticeably distorted out of the O–N(pyridine)–M plane. In the case of (**L1**) TiCl_2 , the anilide and phenoxide arms of the meridional ligand **L1** coordinate in the equatorial plane to put the most π -donating ligand (Cl) in the axial position to maximize the potential for π -donation. In contrast, **1** has the anilide and phenoxide arms in axial positions, since the other ancillary ligands (benzyl groups) do not participate substantially in metal–ligand π -bonding (Figure 3).

Scheme 3. Synthesis of Anilide(Pyridine)Phenoxide Zr and Ti Complexes 1–3

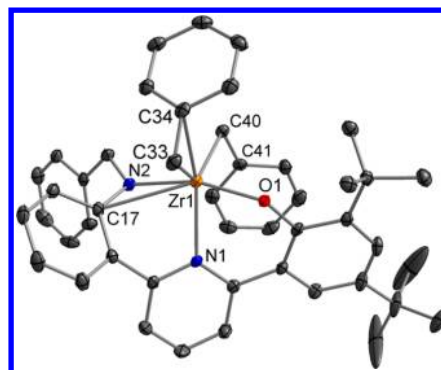
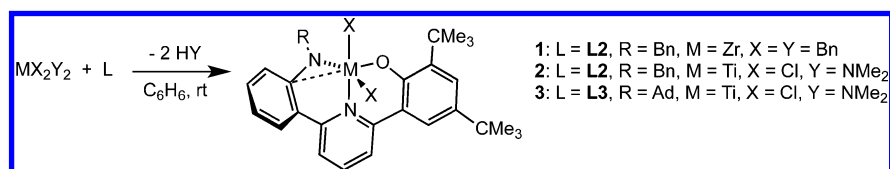


Figure 2. Probability ellipsoid diagram (50%) of the X-ray structure **1**. Selected bond lengths (Å) and angles (deg): Zr(1)–O(1) = 1.9917(7), Zr(1)–N(1) = 2.2911(8), Zr(1)–N(2) = 2.1482(8), Zr(1)–C(17) = 2.8470(9), Zr(1)–C(33) = 2.2913(10), Zr(1)–C(34) = 2.5765(9), Zr(1)–C(40) = 2.2851(9); O(1)–Zr(1)–N(2) = 157.17(3), N(1)–Zr(1)–C(33) = 96.19(3), C(33)–Zr(1)–C(40) = 126.48(3), C(40)–Zr(1)–N(1) = 120.71(3), Zr(1)–C(33)–C(34) = 83.53(5), C(17)–N(2)–Zr(1) = 104.95(6).

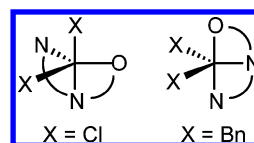


Figure 3. Different binding modes of NNO ligands in trigonal-bipyramidal metal complexes depending on the identity of the X-type ligands.

As has been observed for other early metal dibenzyl complexes,^{6,9,10} one of the benzyl groups in **1** strongly interacts with Zr and is significantly bent toward the metal center to give a Zr(1)–C(33)–C(34)_{ipso} angle of 83.5° and a short Zr(1)–C(34)_{ipso} distance of 2.58 Å.

The molecular structure of **3** was also determined by single crystal X-ray diffraction of crystals grown from slow vapor diffusion of pentane into a concentrated dichloromethane solution of **3** (Figure 4). The structure of **3** is very similar to that obtained for **4** with distorted trigonal-bipyramidal geometry about titanium and very similar bond lengths and angles. Similar to **4**, **3** appears to have an *ipso* interaction with a short Ti(1)–C(17)_{ipso} distance of 2.59 Å and a Ti(1)–N(2)–C(17)_{ipso} angle of 102.8°.

Activation of complexes (**L2**) ZrBn_2 (**1**), (**L2**) TiCl_2 (**2**), and (**L3**) TiCl_2 (**3**) with MAO in toluene or chlorobenzene under 5 atm of propylene at 0 °C resulted in formation of polypropylene (PP). The activity, molecular weight, and polydispersity index (PDI) of the polymers obtained are shown in Table 1. Data for the previously reported compounds (**L1**) ZrBn_2 (**5**) and (**L1**) TiCl_2 (**4**) are included for comparison.⁵ As was observed previously for complexes supported by ligand **L1**, Ti complexes are more active than their Zr congeners with the NNO ligand system. In comparing

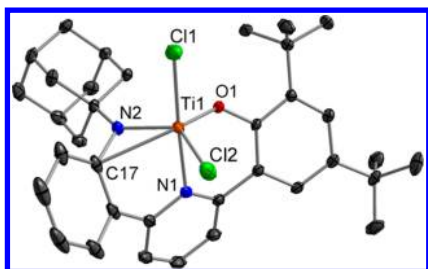


Figure 4. Probability ellipsoid diagram (50%) of the X-ray structure 3. Selected bond lengths (Å) and angles (deg): Ti(1)–O(1) = 1.8293(11), Ti(1)–N(1) = 2.1989(12), Ti(1)–N(2) = 1.8638(11), Ti(1)–Cl(1) = 2.3328(6), Ti(1)–Cl(2) = 2.3023(6), Ti(1)–C(17) = 2.5863(14); O(1)–Ti(1)–N(2) = 112.01(5), O(1)–Ti(1)–Cl(2) = 121.10(3), N(2)–Ti(1)–Cl(2) = 123.85(4), Cl(1)–Ti(1)–N(1) = 176.39(3), C(17)–N(2)–Ti(1) = 102.77(8).

the Ti catalysts with three different anilide R-groups (1-phenylethyl (4), benzyl (2), and adamantyl (3)), 4 was observed to be the most active catalyst and gave the highest molecular weight polymer, although the differences are small. Notably, all of the polymers obtained have narrow PDIs (M_w/M_n), indicating single-site catalysis. The PP from complexes 2 and 3 had no melting points, as expected for stereoirregular PP, and had similar T_g values to those measured for the PP from complexes 5 and 4.

^{13}C NMR spectroscopy was carried out on the polypropylenes obtained with precatalysts 1, 2, and 3. We were particularly interested in comparing the microstructures of the PPs obtained with the Ti catalysts with three different anilide R-groups (achiral 2, achiral 3, and chiral 4). Surprisingly, we observed essentially identical polymer microstructures for all three PPs, as determined by ^{13}C NMR spectroscopy (Figure 5). Whereas there are small differences, all three are stereo- and regioirregular.

These results suggest that—contrary to our original hypothesis—the anilide R-group does not affect the stereo- or regiocontrol of the active polymerization catalyst. This outcome is particularly puzzling considering the uniquely high degree of 2,1-enchainments observed; in fact, no other early metal polymerization catalysts have been reported to produce polypropylene with such a large degree of regioerrors. Although it is conceivable that the anilide R-group is in fact *not* close enough to the incoming monomer to affect monomer selectivity in the putative [(NNO)M–polymeryl/propylene] $^+$ transition state for enchainment, we also considered the possibility that, under the catalytic conditions, all three catalysts are transformed to very similar active catalytic species to

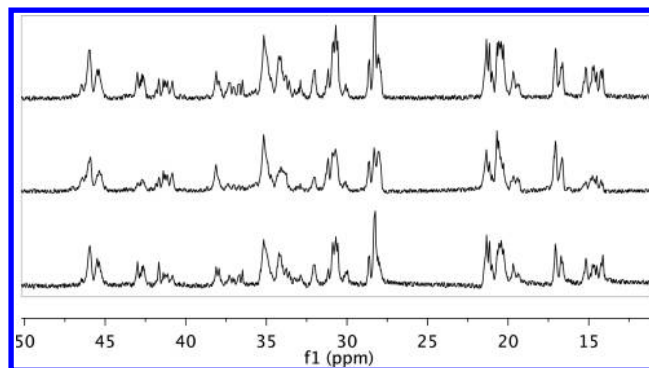


Figure 5. ^{13}C NMR spectra of PP from complex 4 (top), 2 (middle), and 3 (bottom) at 120 °C in $\text{TCE-}d_2$.

account for the very similar regio- and stereocontrol for the different precatalysts. One hypothesis for catalyst modification that could explain the nearly identical regioselectivity for the Ti catalysts 2, 3, and 4 is anilide arm dissociation under polymerization conditions, thus greatly reducing the anilide R-group influence. Notably, bis(anilide)pyridyl polymerization catalysts reported by our group have very large PDIs (4.9–31.2) for propylene polymerization,⁸ which may result from the instability of the Ti–N(anilide) linkages under polymerization conditions; if the Ti–N bonds are susceptible to cleavage, multiple active species may be obtained leading to a broad molecular weight distribution and large PDIs. Admittedly, the NNO polymerization catalysts reported here exhibit narrow PDIs indicative of primarily one active species (Table 1). One would thus need to further postulate that, if the Ti–N(anilide) bonds of the NNO complexes are unstable, the active polymerization catalysts are somehow stabilized by having a phenoxide (rather than another anilide) moiety in the ligand framework.

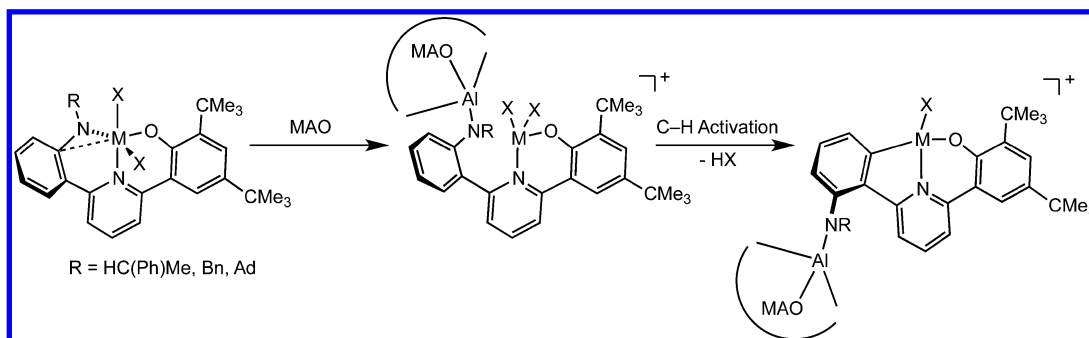
Orthometalated CNO Polymerization Catalyst. In considering the possibility of anilide arm dissociation—perhaps facilitated by MAO—we postulated that the arm could remain uncoordinated or could rotate along the C(aryl)–C(aryl) bond and possibly C–H activate *meta* to the C(aryl)–N(anilide) bond (Scheme 4). Because studying the active catalyst in solution was not feasible, we sought to synthesize model complexes that upon activation with MAO would be analogous to either a labile anilide arm or a C–H-activated anilide arm. Group 4 orthometalated aryl–pyridine–phenoxide (CNO) complexes are well-known and, in fact, have been used in polymerizations of ethylene as well as ethylene/propylene copolymerizations.¹¹

Table 1. Propylene Polymerization Data for Complexes 1–5

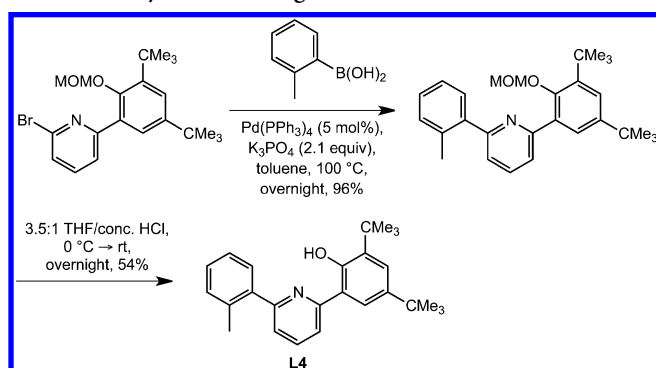
precatalyst	precatalyst (μmol)	time (h)	solvent	yield PP ^a (g)	activity (g PP (mol cat.) $^{-1}$ h $^{-1}$)	T_g (°C)	M_w (g/mol)	M_w/M_n
5	7.6	1	toluene	0.131	1.6×10^4	−8.77	26 000	1.80
4	9.2	0.5	PhCl	0.554	1.2×10^5	−15.25	93 200	1.50
4	9.6	1	PhCl	2.412	2.5×10^5	−14.40	147 000	1.50
4	9.1	3	PhCl	3.963	1.5×10^5	−12.76	401 000	1.99
1	8.1	1	toluene	0.610	3.8×10^4			
2	9.3	0.5	PhCl	0.384	8.3×10^4	−13.66	80 200	1.47
2	9.8	1	PhCl	0.839	8.6×10^4	−13.54	133 000	1.55
2	10.0	3	PhCl	2.504	8.4×10^4	−13.22	197 000	2.38
3	10.2	1	PhCl	0.589	5.8×10^4	−15.36	91 500	1.35

^aPolymerizations were carried out in 30 mL of liquid propylene with 1000 equiv of dry MAO in 3 mL of solvent at 0 °C for the time indicated.

Scheme 4. Potential Pathways for NNO Catalyst Modification upon Activation with MAO

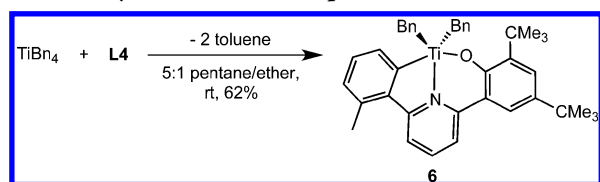


Ligand **L4** was synthesized as shown in Scheme 5. The 2-bromo-6-(3,5-di-*tert*-butyl-2-(methoxymethoxy)phenyl)-

Scheme 5. Synthesis of Ligand **L4**

pyridine synthon reported previously underwent Suzuki coupling with commercially available *o*-tolylboronic acid to form 2-(3,5-di-*tert*-butyl-2-(methoxymethoxy)phenyl)-6-(*o*-tolyl)pyridine.⁵ Deprotection with acidic THF afforded the desired CNO ligand **L4**.

Metalation of **L4** was achieved by reaction with tetrabenzyltitanium to yield orthometalated (**L4**)TiBn₂ **6** (Scheme 6). An

Scheme 6. Synthesis of Ti Complex **6**

X-ray quality crystal of **6** was grown from a 5:1 pentane/ether solution at room temperature, which shows the expected distorted trigonal-bipyramidal structure and bond lengths and angles similar to those reported for crystal structures of other (CNO)TiBn₂ complexes (Figure 6).^{11a} Notably, the Ti(1)–C(27)–C(28)_{ipso} angle for one of the benzyl groups is slightly distorted at 93.5° and has a shortened Ti(1)–C(28)_{ipso} distance of 2.64 Å (compare to 123.6° and 3.17 Å), suggesting a weak η^2 -*ipso* interaction between the benzyl group and Ti.

Activation of **6** with MAO in toluene under 5 atm of propylene at 0 °C yielded PP. The activity of the complex was measured to be 1.5×10^4 g PP (mol cat.)^{−1} h^{−1}, an order of magnitude less active than the NNO-type Ti polymerization catalysts **2**, **3**, and **4**. Importantly, investigation of the PP from **6** with ¹³C NMR spectroscopy revealed stereoirregular and

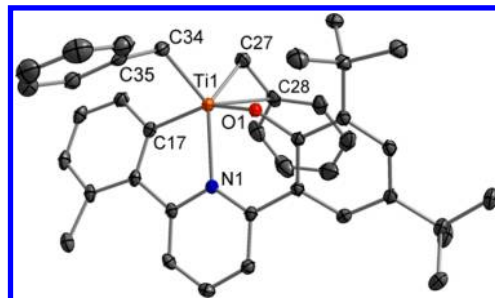


Figure 6. Probability ellipsoid diagram (50%) of the X-ray structure **6**. Selected bond lengths (Å) and angles (deg): Ti(1)–O(1) = 1.8649(4), Ti(1)–N(1) = 2.2132(4), Ti(1)–C(17) = 2.1352(5), Ti(1)–C(27) = 2.1037(6), Ti(1)–C(28) = 2.6385(6), Ti(1)–C(34) = 2.1135(6); O(1)–Ti(1)–C(17) = 153.81(2), C(27)–Ti(1)–C(34) = 97.60(3), C(27)–Ti(1)–N(1) = 126.85(2), C(34)–Ti(1)–N(1) = 134.79(2), Ti(1)–C(27)–C(28) = 93.46(4).

regioregular PP (Figure 7). This result tentatively suggests that the NNO complexes do not C–H activate to form CNO polymerization catalysts.

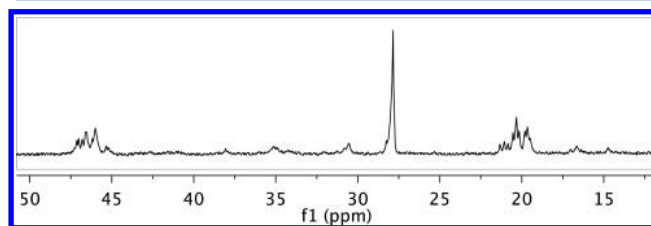
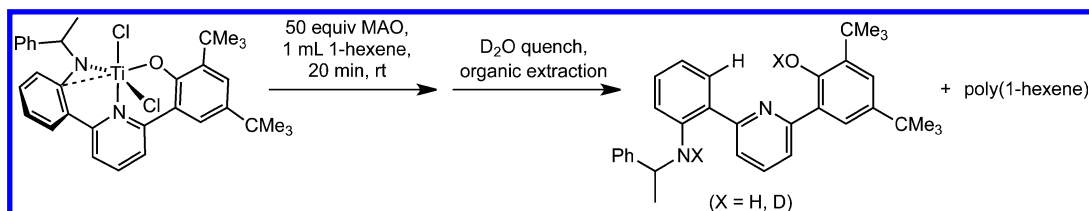


Figure 7. ¹³C NMR spectrum of stereoirregular regioregular PP from complex **6** at 120 °C in TCE-*d*₂.

To further investigate the possibility of C–H activation, a solution of **4** in chlorobenzene was activated with 50 equiv of MAO in the presence of 1-hexene.¹² The solution of precatalyst **4**, MAO, and 1-hexene was stirred for 20 min and then quenched with D₂O. The organic layer was extracted and analyzed by ¹H NMR spectroscopy, which revealed the formation of poly(1-hexene) and recovery of the intact ligand **L1** (Scheme 7). If C–H activation had occurred under the polymerization conditions, deuterium incorporation into the 6-position of the anilide aryl ring would be expected; however, the ligand isolated after D₂O quenching had only H at this position (HRMS or ¹H NMR). Moreover, the anilide 1-phenylethyl R-group of the NNO ligand **L1** was intact, ruling out N–C bond cleavage (possibly by MAO) as another potential pathway for catalyst modification. Finally, monomer was not incorporated into the isolated ligand, as has been

Scheme 7. Recovery of Intact Ligand L1 after Activation and Polymerization of 1-Hexene with Complex 4



observed for Hf pyridyl–amide catalysts.¹³ On the basis of these experiments, we have tentatively ruled out (1) C–H activation of the anilide arm to form a $\{(CNO)Ti\}$ complex, (2) N–C bond cleavage of the anilide R-group, and (3) monomer insertion into M–ligand bonds to explain the nearly identical regiocontrol observed for these NNO-type polymerization catalysts.¹⁴

Propylene Polymerizations with Different Activators at Variable Pressures and Temperatures. Our studies with various post-metallocene polymerization catalysts up to this point suggest that group 4 complexes with anilide(pyridine)–phenoxide (NNO) ligands display a lack of regioselectivity for α -olefin polymerization with the intact NNO ligand coordinated and that this regioselectivity is inherent in the catalyst structure in a manner not yet defined. We therefore examined these catalysts systems under different polymerization reaction conditions to investigate whether temperature, pressure, or cocatalyst/activator had any effect on regioselectivity.

Titanium complex 4 was tested in a 1 L glass reactor at King Fahd University of Petroleum and Minerals (KFUPM), which allowed for carrying out propylene polymerizations at higher temperatures (room temperature to about 50 °C) and higher pressures (8–9 atm), compared to the standard Fisher–Porter setup (0 °C, 5 atm). A polymerization run with 36 mg of precatalyst 4 at 6 atm and 25 °C using 40 mL of toluene, ca. 100 mL of propylene, 1000 equiv of MAO, and 33 equiv of triisobutylaluminum (TIBA) yielded very sticky polypropylene (estimated activity of 10^6 g PP (mol cat.)^{−1} h^{−1}). ¹³C NMR spectroscopy of the polymer (Figure 8) revealed a somewhat

different, but still largely regioirregular microstructure than that obtained under the conditions used previously (Table 1). Part of the reason for this difference could be attributed to the addition of TIBA in the KFUPM run. An additional run therefore was carried out with 4 in chlorobenzene using modified MAO (MMAO) at 0 °C and 5 atm. Indeed, with MMAO as a cocatalyst, a sticky PP was obtained with activity determined to be 1.0×10^5 g PP (mol cat.)^{−1} h^{−1}. ¹³C NMR spectroscopy on the PP from the reaction of 4/MMAO revealed a microstructure very similar to that from the PP synthesized at KFUPM with 4/MAO/TIBA (Figure 8). These results suggest that the polymerization reaction is sensitive to the aluminoxane activator but importantly show that the regiorandom behavior of catalyst 4 is not significantly affected by reaction temperatures between 0 and 25 °C.

GPC of the polymer obtained from 4/MAO/TIBA at KFUPM revealed lower molecular weight ($M_w = 4080$ g/mol; $T_g = -26.11$ °C) compared to the polymers obtained in the Fisher–Porter setup with the same precatalyst under different polymerization conditions (Table 1), although the PDI (2.45) is still rather narrow. The GPC of PP from 4/MMAO run at 0 °C showed a bimodal distribution with a low molecular weight peak of 3980 g/mol and a high molecular weight peak of 195 400 g/mol. The low molecular weight polymers observed in polymerizations with 4/MAO/TIBA and 4/MMAO may be due, at least in part, to free alkylaluminum present in the system, as aluminum alkyls are known to act as chain-transfer agents;¹⁵ only higher molecular weight PP was obtained when dry MAO with minimal free trimethylaluminum (TMA) was used (Table 1).

Ti complex 4 was also tested for propylene polymerization in a 1.8 L stainless steel batch reactor. Polymerizations were run at 70 °C with 700 g of IsoparE, 150 g of propylene, and 50 psi of hydrogen for 15 min. PMAO-IP or MAO was used as a cocatalyst. These polymerizations yielded solid PP with excellent activities of 2.1×10^6 g PP (mol cat.)^{−1} h^{−1} (4/PMAO-IP) and 9.6×10^5 g PP (mol cat.)^{−1} h^{−1} (4/MAO) (Table 2) and broad molecular weight distributions, M_w/M_n , of 18.6 and 20.9, respectively; however, the GPC traces show trimodal distributions. Deconvolution of the GPC data for the PP from 4/PMAO-IP reveals two low- M_w peaks of 320 and 1860 g/mol and a high- M_w peak of 85 880 g/mol. Similarly, the deconvoluted GPC data for 4/MAO has two low- M_w peaks of 320 and 2360 g/mol and a high- M_w peak of 82 260 g/mol. Most interestingly, unlike the PP produced by our catalysts

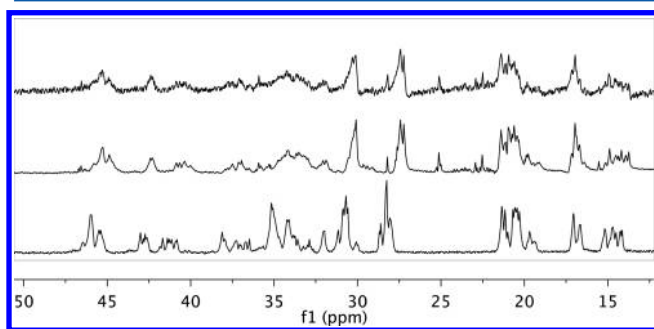


Figure 8. ¹³C NMR spectra of PP from complex 4/MAO/TIBA run at 25 °C at KFUPM (top), PP from 4/MMAO under conditions used in Table 1 (middle), and PP from 4/dry MAO under conditions used in Table 1 (bottom). Spectra were taken at 120 °C in TCE-*d*₂.

Table 2. Propylene Polymerization Data for 4/PMAO-IP and 4/MAO

precatalyst	precatalyst (mmol)	time (h)	MAO (equiv)	PMAO-IP (equiv)	yield PP ^a (g)	activity (g PP (mol cat.) ^{−1} h ^{−1})	<i>T</i> _g (°C)	<i>T</i> _m (°C)	<i>M</i> _w (g/mol)	<i>M</i> _w / <i>M</i> _n
4	0.010	0.25		10 000	5.3	2.1×10^6	−12.8	158.2	65 600	18.55
4	0.010	0.25	10 000		2.4	9.6×10^6	−31.0	155.3	50 000	20.86

^aPolymerizations were carried out with 700 g of IsoparE, 150 g of propylene, and 50 psi of hydrogen at 70 °C for the time indicated.

under any other condition, the PP produced with 4/PMAO-IP or 4/MAO had melting points of 158.2 and 155.3 °C, which is in the range expected for isotactic PP (Table 2).

Indeed, ^{13}C NMR spectroscopy on the polymers revealed peaks indicative of isotactic PP (iPP) as well as peaks for stereoirregular and regioirregular PP (Figures 9 and 10);

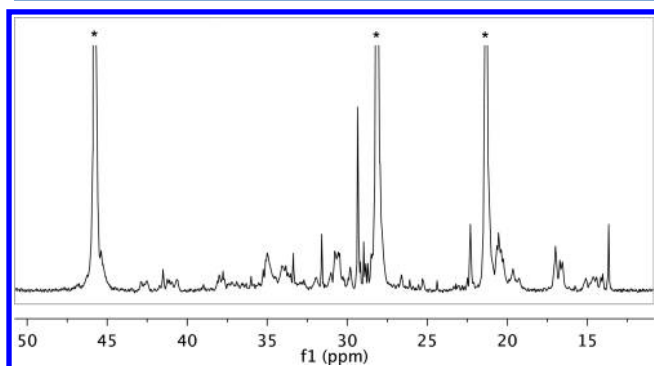


Figure 9. ^{13}C NMR spectrum of PP from 4/PMAO-IP at 115 °C in TCE-d_2 . Resonances for iPP are indicated with asterisks.

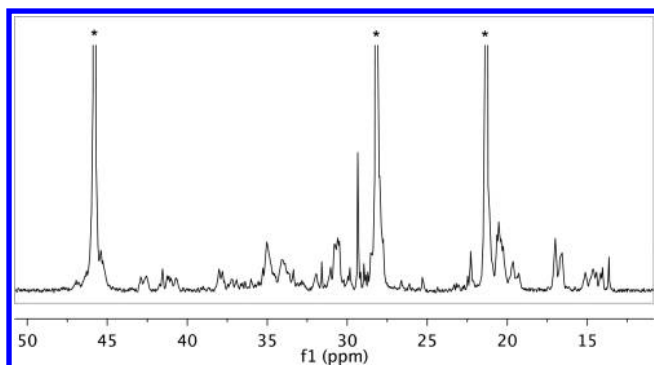


Figure 10. ^{13}C NMR spectrum of PP from 4/MAO at 115 °C in TCE-d_2 . Resonances for iPP are indicated with asterisks.

significantly, these results provide the first example of isotactic PP from an anilide(pyridine)phenoxide type precatalyst. Related phenoxide(pyridine)amido and phenoxide(thiazole)-amido precatalysts have been reported that also give iPP under slightly different polymerization conditions.¹⁶ Consistent with the GPC data, the ^{13}C NMR spectra suggest that more than one type of polymer was made (presumably by different active species). Comparison of the ^{13}C NMR spectra for PP from 4/PMAO-IP or 4/MAO to the PP from 4, 2, or 3 activated with dry MAO shows identical regioirregular microstructures.

These results seem to indicate that at least one new species is obtained from 4 under these polymerization conditions, which polymerizes propylene with high stereo- and regioselectivity to yield iPP. At the same time, however, the species which was observed to yield regioirregular and stereoirregular PP at 0 or 22 °C is still active.

3. CONCLUSIONS

A series of asymmetric post-metallocene group 4 complexes based on a modular anilide(pyridine)phenoxide (NNO) framework have been synthesized and tested for propylene polymerization activity. In most cases, the complexes were found to polymerize propylene upon activation with MAO with moderate to good activities. Interestingly, these complexes

produce highly regioirregular (and stereoirregular) polypropylene resulting from little apparent preference by these catalysts for 1,2- or 2,1-insertions of propylene. Significantly, near-regionrandom behavior is highly unusual for early metal polymerization catalysts, which typically polymerize propylene with a very high degree of (normally 1,2-) regiocontrol. Subjecting the anilide(pyridine)phenoxide catalyst 4 to different polymerization conditions, namely higher pressures of propylene and higher reaction temperatures, revealed that the catalytically active species that produces regioirregular PP operates regardless of temperature or pressure but also that at least one new polymerization species is formed at 70 °C under dihydrogen, which, surprisingly, produces isotactic PP.

It is our belief that these results point to some form of catalyst modification upon activation, which at this time remains to be fully elucidated. Although these experiments together do not provide a satisfying explanation of the unusual polymerization behavior of group 4 anilide(pyridine)phenoxide complexes, they represent a small contribution to our understanding of the complex behavior of post-metallocene catalysts. As recently noted by Busico, “the common belief that “single-site” olefin polymerization catalysis is easily amenable to rational understanding” does not hold true for post-metallocene catalysts, and in fact, “it is clear that molecular catalysts are not necessarily simple nor foreseeable.”¹⁷ Nonetheless, these results importantly show that new discoveries are still possible in established fields like early metal α -olefin polymerization catalysis. Continued work in this area will undoubtedly lead to new breakthroughs in post-metallocene catalysts for olefin polymerization.

4. EXPERIMENTAL SECTION

General Considerations and Instrumentation. All air- and moisture-sensitive compounds were manipulated using standard high-vacuum and Schlenk techniques or manipulated in a glovebox under a nitrogen atmosphere. Solvents for air- and moisture-sensitive reactions were dried over sodium benzophenone ketyl and stored over “titanocene”¹⁸ where compatible or dried by the method of Grubbs.¹⁹ $\text{TiCl}_2(\text{NMe}_2)_2$,²⁰ ZrBn_4 ,²¹ and $(\text{NNO})\text{TiCl}_2$ (4)⁵ were prepared following literature procedures. Methylaluminoxane (MAO) was purchased as a toluene solution from Albemarle and was dried in vacuo at 150 °C overnight to remove free trimethylaluminum before use. Propylene was dried by passage through a column of activated alumina and molecular sieves. Benzene- d_6 , toluene- d_8 , $\text{C}_6\text{D}_5\text{Cl}$, and 1,1,2,2-tetrachloroethane- d_2 (TCE-d_2) were purchased from Cambridge Isotopes. Benzene- d_6 and toluene- d_8 were dried over sodium benzophenone ketyl then over titanocene. $\text{C}_6\text{D}_5\text{Cl}$ was distilled from CaH_2 and passed through a plug of activated alumina prior to use. NMR spectra were recorded on Varian Mercury 300, Varian INOVA 500, or Varian INOVA 600 spectrometers and referenced to the solvent residual peak. High-resolution mass spectra (HRMS) were obtained at the California Institute of Technology Mass Spectral Facility using a JEOL JMS-600H magnetic sector mass spectrometer. Elemental analyses were performed by Midwest Microlab LLC (Indianapolis, IN) or Robertson Microlit Laboratories, Inc. (Ledgewood, NJ). X-ray quality crystals were grown as indicated in the experimental procedures for each complex. The crystals were mounted on a glass fiber with Paratone-N oil. Data collection was carried out on a Bruker KAPPA APEX II diffractometer with a 0.710 73 Å Mo $K\alpha$ source. Structures were determined using direct methods with standard Fourier techniques using the Bruker AXS software package. In some cases, Patterson maps were used in place of the direct methods procedure. Some details regarding crystal data and structure refinement are available in the Supporting Information. Selected bond lengths and angles are supplied in the corresponding figures of the paper.

(L2)ZrBn₂ 1. A 2 mL benzene solution of **L2-H₂** (66.5 mg, 0.143 mmol) was added to a 2 mL benzene solution of ZrBn₄ (65.0 mg, 0.143 mmol) and stirred for 10 min under an inert atmosphere in the glovebox. Benzene was removed in vacuo from the resulting yellow solution to yield a yellow oil, which was redissolved in pentane and pumped dry several times to remove residual toluene to reveal a yellow powder. (90.8 mg, 0.123 mmol, yield: 86%). ¹H NMR (500 MHz, toluene-*d*₈) δ: 1.40 (s, 9H, C(CH₃)₃), 1.64 (s, 9H, C(CH₃)₃), 2.06 (d, *J* = 10.2 Hz, 2H, Zr-CH₂), 2.22 (d, *J* = 10.3 Hz, 2H, Zr-CH₂), 4.85 (s, 2H, NCH₂Ph), 6.64–6.74 (m, 7H, aryl-CH), 6.77–6.81 (m, 1H, aryl-CH), 6.80–6.89 (m, 11H, aryl-CH), 7.07 (dd, *J* = 7.9, 1.6 Hz, 1H, aryl-CH), 7.25 (ddd, *J* = 8.5, 7.1, 1.6 Hz, 1H, aryl-CH), 7.35 (dd, *J* = 8.2, 1.2 Hz, 1H, aryl-CH), 7.40 (d, *J* = 2.3 Hz, 1H, aryl-CH), 7.60 (d, *J* = 2.2 Hz, 1H, aryl-CH). ¹³C NMR (126 MHz, toluene-*d*₈) δ: 30.90 (C(CH₃)₃), 32.24 (C(CH₃)₃), 34.97 (C(CH₃)₃), 36.14 (C(CH₃)₃), 55.96 (NCH₂), 65.65 (ZrCH₂), 121.70, 121.92, 122.33, 122.38, 123.75, 124.91, 125.00, 126.94, 127.35, 127.58, 127.92, 128.08, 128.67, 129.59, 131.74, 133.00, 138.49, 138.96, 140.76, 141.64, 142.29, 143.84, 156.24, 156.30, 157.26 (aryl-C). Anal. Calcd for C₄₆H₄₈N₂OZr (%): C, 75.06; H, 6.57; N, 3.81. Found (1): C, 68.19; H, 6.23; N, 3.79. (2) C, 66.65; H, 6.08; N, 4.24. (This compound is air- and moisture-sensitive, and despite repeated attempts satisfactory analysis could not be obtained.)

(L2)TiCl₂ 2. A 3 mL benzene solution of **L2-H₂** (60.4 mg, 0.130 mmol) was added to a 3 mL benzene solution of TiCl₂(NMe₂)₂ (26.9 mg, 0.131 mmol) and stirred for 10 min under an inert atmosphere in the glovebox. Benzene was removed in vacuo from the resulting dark red solution to yield a deep purple solid, which was triturated several times with pentane to remove free dimethylamine (77.6 mg, 0.133 mmol, quantitative yield). ¹H NMR (300 MHz, C₆H₅Cl) δ: 1.30 (s, 9H, C(CH₃)₃), 1.66 (s, 9H, C(CH₃)₃), 4.95 (s, 1H, NCH₂), 6.12 (s, 1H, NCH₂), 6.60–6.85 (m, 6H, aryl-CH), 7.02–7.12 (m, 2H, aryl-CH), 7.17 (dd, *J* = 7.8, 1.0 Hz, 1H, aryl-CH), 7.25–7.34 (m, 1H, aryl-CH), 7.48 (t, *J* = 8.0 Hz, 1H, aryl-CH), 7.56 (dd, *J* = 8.0, 1.5 Hz, 1H, aryl-CH), 7.63–7.72 (m, 3H, aryl-CH). ¹³C NMR (126 MHz, C₆D₅Cl, –15 °C) δ: 31.41 C(CH₃)₃, 32.45 (C(CH₃)₃), 35.69 (C(CH₃)₃), 36.63 C(CH₃)₃, 117.29, 123.11, 123.98, 126.02, 128.18, 129.55, 130.64, 132.98, 138.48, 139.58, 139.67, 145.83, 153.52, 155.43, 159.48 (aryl-C). Anal. Calcd for C₃₂H₃₄Cl₂N₂O₂Ti (%): C, 66.11; H, 5.89; N, 4.82. Found: C, 65.98; H, 6.06; N, 4.87.

(L3)TiCl₂ 3. A 3 mL benzene solution of **L3-H₂** (67.6 mg, 0.133 mmol) was added to a 3 mL benzene solution of TiCl₂(NMe₂)₂ (27.5 mg, 0.133 mmol) and stirred for 10 min under inert atmosphere in the glovebox. Benzene was removed in vacuo from the resulting dark red solution to yield a light orange solid, which was triturated several times with pentane to remove free dimethylamine (86.4 mg, 0.134 mmol, quantitative yield). ¹H NMR (500 MHz, C₆D₅Cl) δ: 1.30 (s, 9H, C(CH₃)₃), 1.33–1.39 (m, Ad-CH₂, 6H), 1.63–1.71 (m, 6H, Ad-CH₂), 1.78 (s, 9H, C(CH₃)₃), 1.79 (br s, 3H, Ad-CH), 7.24 (dd, *J* = 7.7, 1.0 Hz, 1H, aryl-CH), 7.36–7.43 (m, 2H, aryl-CH), 7.48–7.55 (m, 2H, aryl-CH), 7.58–7.62 (m, 1H, aryl-CH), 7.71 (q, *J* = 2.4 Hz, 2H, aryl-CH), 7.77 (dd, *J* = 8.3, 1.1 Hz, 1H, aryl-CH). ¹³C NMR (126 MHz, C₆D₅Cl) δ: 29.93 (Ad-CH), 30.36 (C(CH₃)₃), 31.31 (C(CH₃)₃), 34.60 (C(CH₃)₃), 35.69 (C(CH₃)₃), 35.87 (Ad-CH₂), 42.62 (Ad-CH₂), 69.51 (Ad-quat), 122.09, 122.25, 123.34, 123.72, 127.83, 128.65, 130.31, 131.13, 132.03, 133.17, 134.16, 137.90, 139.15, 144.77, 152.18, 153.39, 158.07 (aryl-C). Anal. Calcd for C₃₅H₄₂Cl₂N₂O₂Ti (%): C, 67.21; H, 6.77; N, 4.48. Found (1): C, 66.53; H, 6.80; N, 4.20. (2) C, 66.37; H, 6.73; N, 4.36. (This compound is air- and moisture-sensitive, and despite repeated attempts satisfactory %C analysis could not be obtained.)

(L4)TiBn₂ 6. To a stirring slurry of **L4-H₂** (30.2 mg, 0.081 mmol) in 5:1 pentane/ether was added to a 3 mL solution of TiBn₄ (33.4 mg, 0.081 mmol), and the resulting red solution was stirred for 10 min under an inert atmosphere in the glovebox. The reaction solution was passed through a pad of Celite to remove impurities and with 5:1 pentane/ether, and then solvent was removed in vacuo to yield a dark red solid, which was triturated several times with pentane before being redissolved in 5:1 pentane/ether and recrystallized by cooling in the freezer (30.2 mg, 0.050 mmol, 62% yield). ¹H NMR (300 MHz,

toluene-*d*₈) δ: 1.37 (s, 9H, C(CH₃)₃), 1.85 (s, 9H, C(CH₃)₃), 2.21 (s, 3H, Ar-CH₃), 3.88 (d, *J* = 8.3 Hz, 2H, Ti-CH₂), 4.15 (d, *J* = 8.3 Hz, 2H, Ti-CH₂), 6.33–6.44 (m, 2H, aryl-CH), 6.54 (t, *J* = 7.7 Hz, 4H, aryl-CH), 6.63–6.71 (m, 4H, aryl-CH), 6.82 (d, *J* = 4.7 Hz, 2H, aryl-CH), 7.13 (d, *J* = 5.4 Hz, 1H, aryl-CH), 7.23 (t, *J* = 7.1 Hz, 1H, aryl-CH), 7.37 (d, *J* = 2.4 Hz, 1H, aryl-CH), 7.69 (d, *J* = 2.4 Hz, 1H, aryl-CH), 8.51 (d, *J* = 6.9 Hz, 1H, aryl-CH). ¹³C NMR (126 MHz, C₆D₆) δ: 23.59 (tolyl-CH₃), 30.99 (C(CH₃)₃), 31.84 (C(CH₃)₃), 34.66 (C(CH₃)₃), 35.80 (C(CH₃)₃), 92.42 (Ti-CH₂), 119.61, 121.77, 123.32, 124.72, 125.70, 126.58, 127.75, 128.57, 129.33, 131.13, 132.54, 132.65, 133.00, 136.76, 137.81, 138.66, 142.08, 157.60, 158.15, 165.17, 204.42 (aryl-C). Anal. Calcd for C₄₀H₄₃NOTi (%): C, 79.85; H, 7.20; N, 2.33. Found (1): C, 74.91; H, 6.99; N, 2.33. (2) C, 74.74; H, 6.86; N, 2.32. (This compound is air- and moisture-sensitive, and despite repeated attempts satisfactory %C analysis could not be obtained.)

Recovery of Ligand L1 from Small Scale Polymerization Reaction with 4 and 1-Hexene. To a 20 mL vial in the glovebox was added 1 mL of 1-hexene and 50 equiv (0.193 g) of dry MAO. The 1-hexene/MAO solution was stirred for 5 min, then a solution of **4** dissolved in 1 mL of PhCl was added to the vial, and the reaction was stirred for 25 min at room temperature. The vial was then removed from the glovebox, and 2 mL of D₂O was added slowly, followed by 5 drops of concentrated HCl and 4 mL of D₂O, which resulted in decolorization of the dark red solution. The organic layer was extracted with hexanes (3 × 4 mL), and the combined organics were dried over magnesium sulfate and solvent removed in vacuo to reveal a pale yellow solid. 44.9 mg (**L1-D₂** and poly(1-hexene)). MS (FAB+) *m/z*: calcd for C₃₃H₃₈ON₂ [M]⁺ 478.2984; found 478.3524.

General Polymerization Protocol. A high-pressure glass reactor was charged with solid MAO (1000 equiv), and 2.3 mL of toluene (distilled from “Cp₂TiH₂”) was added. The vessel was attached to a propylene tank and evacuated, and propylene (~30 mL) was condensed in upon cooling to 0 °C. The appropriate precatalysts was added as a solution (toluene or chlorobenzene, 0.7 mL) via syringe. The reaction mixture was stirred vigorously at 0 °C for the desired amount of time, excess propylene was (carefully) vented, and a 10% solution of HCl/MeOH (50 mL) was added slowly to quench the reaction. The resulting mixture was transferred to an Erlenmeyer flask and stirred at room temperature overnight. The precipitated polymer was collected and washed with methanol (3 × 10 mL), evacuated to remove solvent, further dried under high vacuum for 12 h, and examined by NMR spectroscopy, GPC, and DSC. ¹³C NMR spectra were acquired at 120 °C in tetrachloroethane, using a 2 s relaxation delay with a 2.3 s acquisition time.

■ ASSOCIATED CONTENT

● Supporting Information

Experimental details including characterization of new compounds and experimental procedures; crystallographic data. This material is available free of charge via the Internet at <http://pubs.acs.org>.

■ AUTHOR INFORMATION

Corresponding Authors

*E-mail jal@caltech.edu (J.A.L.).

*E-mail bercaw@caltech.edu (J.E.B.).

Notes

The authors declare no competing financial interest.

■ ACKNOWLEDGMENTS

The authors gratefully acknowledge the USDOE Office of Basic Energy Sciences (DE-FG03-85ER13431 to J.E.B.) for funding. An NSF-GRF to R.C.K. is gratefully acknowledged. We thank Larry Henling, Dr. Michael Takase, and Dr. Wojciech Bury for assistance with X-ray crystallography.

■ REFERENCES

- (1) Hustad, P. D. *Science* **2009**, *325*, 704–707.
- (2) Natta, G.; Pino, P.; Corradini, P.; Danusso, F.; Mantica, E.; Mazzanti, G.; Moraglio, G. *J. Am. Chem. Soc.* **1955**, *77*, 1708–1710.
- (3) (a) Brintzinger, H. H.; Fischer, D.; Mülhaupt, R.; Rieger, B.; Waymouth, R. M. *Angew. Chem., Int. Ed.* **1995**, *34*, 1143–1170. (b) Coates, G. W. *Chem. Rev.* **2000**, *100*, 1223–1252. (c) Resconi, L.; Cavallo, L.; Fait, A.; Piemontesi, F. *Chem. Rev.* **2000**, *100*, 1253–1346.
- (4) (a) Domski, G. J.; Rose, J. M.; Coates, G. W.; Bolig, A. D.; Brookhart, M. *Prog. Polym. Sci.* **2007**, *32*, 30–92. (b) Anderson-Wile, A. M.; Edson, J. B.; Coates, G. W. In *Complex Macromolecular Architectures*; John Wiley & Sons (Asia) Pte Ltd.: Singapore, 2011; pp 267–316.
- (5) Klet, R. C.; VanderVelde, D. G.; Labinger, J. A.; Bercaw, J. E. *Chem. Commun.* **2012**, *48*, 6657–6659.
- (6) Agapie, T.; Henling, L. M.; DiPasquale, A. G.; Rheingold, A. L.; Bercaw, J. E. *Organometallics* **2008**, *27*, 6245–6256.
- (7) Golisz, S. R.; Bercaw, J. E. *Macromolecules* **2009**, *42*, 8751–8762.
- (8) Tonks, I. A.; Tofan, D.; Weintrob, E. C.; Agapie, T.; Bercaw, J. E. *Organometallics* **2012**, *31*, 1965–1974.
- (9) Bassi, I.; Allegra, G.; Scordamaglia, R.; Chioccola, G. *J. Am. Chem. Soc.* **1971**, *93*, 3787–3788.
- (10) Giesbrecht, G. R.; Whitener, G. D.; Arnold, J. *Organometallics* **2000**, *19*, 2809–2812.
- (11) (a) Chan, M. C.; Kui, S. C.; Cole, J. M.; McIntyre, G. J.; Matsui, S.; Zhu, N.; Tam, K. H. *Chem.—Eur. J.* **2006**, *12*, 2607–2619. (b) Tam, K.-H.; Lo, J. C.; Guo, Z.; Chan, M. C. *J. Organomet. Chem.* **2007**, *692*, 4750–4759. (c) Tam, K.-H.; Chan, M. C.; Kaneyoshi, H.; Makio, H.; Zhu, N. *Organometallics* **2009**, *28*, 5877–5882. (d) Liu, C.-C.; So, L.-C.; Lo, J. C.; Chan, M. C.; Kaneyoshi, H.; Makio, H. *Organometallics* **2012**, *31*, 5274–5281. (e) Lo, J. C.; Chan, M. C.; Lo, P.-K.; Lau, K.-C.; Ochiai, T.; Makio, H. *Organometallics* **2013**, *32*, 449–459.
- (12) We have separately demonstrated that **4** polymerizes 1-hexene to make stereoirregular and regioirregular poly(1-hexene): Klet, R. C. Ph.D. Thesis, California Institute of Technology, 2013.
- (13) (a) Boussie, T. R.; Diamond, G. M.; Goh, C.; Hall, K. A.; LaPointe, A. M.; Leclerc, M. K.; Murphy, V.; Shoemaker, J. A.; Turner, H.; Rosen, R. K.; Stevens, J. C.; Alfano, F.; Busico, V.; Cipullo, R.; Talarico, G. *Angew. Chem., Int. Ed.* **2006**, *45*, 3278–3283. (b) Froese, R. D.; Hustad, P. D.; Kuhlman, R. L.; Wenzel, T. T. *J. Am. Chem. Soc.* **2007**, *129*, 7831–7840.
- (14) The conclusions reached from the results of these experiments assume that the majority of the precatalyst is activated with MAO and participates in catalysis prior to addition of water.
- (15) (a) Resconi, L.; Bossi, S.; Abis, L. *Macromolecules* **1990**, *23*, 4489–4491. (b) Chien, J. C. W.; Wang, B. P. *J. Polym. Sci., Part A: Polym. Chem.* **1988**, *26*, 3089–3102. (c) Chien, J. C. W.; Razavi, A. *J. Polym. Sci., Part A: Polym. Chem.* **1988**, *26*, 2369–2380. (d) Chien, J. C. W.; Wang, B. P. *J. Polym. Sci., Part A: Polym. Chem.* **1990**, *28*, 15–38.
- (16) The polymerization conditions were as follows: toluene, 100 psi of propylene, 75 °C, and $[\text{PhNMe}_2\text{H}]^+[\text{B}(\text{C}_6\text{F}_5)_4]^-$ was used as the activator in combination with diisobutylaluminum as an alkylator. See: Diamond, G. M.; Hall, K. A.; LaPointe, A. M.; Leclerc, M. K.; Longmire, J.; Shoemaker, J. A.; Sun, P. *ACS Catal.* **2011**, *1*, 887–900.
- (17) Busico, V.; Cipullo, R.; Pellecchia, R.; Rongo, L.; Talarico, G.; Macchioni, A.; Zuccaccia, C.; Froese, R. D. J.; Hustad, P. D. *Macromolecules* **2009**, *42*, 4369–4373.
- (18) Burger, B. J.; Bercaw, J. E. *ACS Symp. Ser.* **1987**, *357*, 79–115.
- (19) Pangborn, A. B.; Giardello, M. A.; Grubbs, R. H.; Rosen, R. K.; Timmers, F. J. *Organometallics* **1996**, *15*, 1518–1520.
- (20) Benzing, E.; Kornicker, W. *Chem. Ber.* **1961**, *94*, 2263–2267.
- (21) Felten, J. J.; Anderson, W. P. *J. Organomet. Chem.* **1972**, *36*, 87–92.